

Hidden-bottom hadronic decays of $\Upsilon(10753)$ with a $\eta^{(\prime)}$ or ω emission

Yu-Shuai Li^{1,2,*}, Zi-Yue Bai^{1,2,†}, Qi Huang^{3,4,‡} and Xiang Liu^{1,2,4,§¶}

¹*School of Physical Science and Technology, Lanzhou University, Lanzhou 730000, China*

²*Research Center for Hadron and CSR Physics, Lanzhou University and Institute of Modern Physics of CAS, Lanzhou 730000, China*

³*University of Chinese Academy of Sciences (UCAS), Beijing 100049, China*

⁴*Lanzhou Center for Theoretical Physics and Frontier Science Center for Rare Isotopes, Lanzhou University, Lanzhou 730000, China*

In this work, we propose the $4S$ - $3D$ mixing scheme to assign the $\Upsilon(10753)$ into the conventional bottomonium family. Under this interpretation, we further study its hidden-bottom hadronic decays with a $\eta^{(\prime)}$ or ω emission, which include $\Upsilon(10753) \rightarrow \Upsilon(1S)\eta^{(\prime)}$, $\Upsilon(10753) \rightarrow h_b(1P)\eta$ and $\Upsilon(10753) \rightarrow \chi_{bJ}\omega$ ($J=0,1,2$) processes. Since the $\Upsilon(10753)$ is above the $B\bar{B}$ threshold, the coupled-channel effect cannot be ignored, thus, when calculating partial decay widths of these $\Upsilon(10753)$ hidden-bottom decays, we apply the hadronic loop mechanism. Our result shows that these discussed decay processes own considerable branching fractions with the order of magnitude of $10^{-4} \sim 10^{-3}$, which can be accessible at Belle II and other future experiments.

I. INTRODUCTION

When checking the status of the bottomonia collected in Particle Data Group (PDG) [1], it is easy to find that compared with charmonium family, bottomonium family is far from been established. Until now, above the $B\bar{B}$ threshold, experiments have only observed three vector bottomonia $\Upsilon(10580)$, $\Upsilon(10860)$ and $\Upsilon(11020)$. Thus, to construct bottomonium family, finding more bottomonia is a crucial step. Along this line, the Belle and further Belle II experiments are playing important roles in exploring new bottomonium [2].

Recently, the Belle Collaboration reanalyzed the cross section of $e^+e^- \rightarrow \Upsilon(nS)\pi^+\pi^-$ ($n = 1, 2, 3$) and updated their measurements to supersede the previous result [3, 4]. In their new analysis, apart from the already known resonances $\Upsilon(10860)$ and $\Upsilon(11020)$ [4–9], a new structure near 10.75 GeV, which is refereed to be $\Upsilon(10753)$ in PDG [1], appears in the $\Upsilon(nS)\pi^+\pi^-$ ($n = 1, 2, 3$) invariant mass spectrum, whose mass and width are fitted as $M = (10752.7 \pm 5.9^{+0.7}_{-1.1})$ MeV and $\Gamma = (35.5^{+17.6+3.9}_{-11.3-3.3})$ MeV, respectively. Additionally, its spin-parity is indicated to be $J^{PC} = 1^{--}$ by the requirement of the production processes. This new reported bottomonium-like structure quickly inspired theorist's interests in revealing its inner structure, where the conventional bottomonium state assignment [10, 11] and several exotic state interpretations, which include tetraquark state [12, 13] and hybrid state [14, 15], and kinetic effect [16, 17] were proposed.

When treating the $\Upsilon(10753)$ as a conventional bottomonium state, we have to face a serious problem. The calculation of the mass spectrum of bottomonium family [19–23] shows that the predicted masses of $\Upsilon(4S)$, $\Upsilon(3D)$, $\Upsilon(5S)$ and $\Upsilon(4D)$ are around (10607 – 10640) MeV, (10653 – 10717) MeV, (10818 – 10878) MeV and (10853 – 10928) MeV, respectively. Obviously, the mass of the observed $\Upsilon(10753)$ can not fall into these predicted mass ranges, which is the diffi-

culty to assign the $\Upsilon(10753)$ to be a bottomonium state. Naturally, the exotic state explanations [12–15] were given since this mass problem can be solved by this way.

In fact, we should mention some experiences on constructing the charmonium family. In Ref. [24], in order to understand the puzzling phenomenon involved in the $\psi(3686)$ and $\psi(3770)$, Rosner introduced the $2S$ and $1D$ state mixing scheme. Furthermore, when checking the higher charmonia, such effect also should be emphasized. In Ref. [25], the predicted masses of $\psi(4S)$ and $\psi(3D)$ are 4274 MeV and 4334 MeV respectively. If assigning the $Y(4220)$ [1] as a $\psi(4S)$ charmonium state, the mass of $\psi(4S)$ is about 54 MeV higher than the mass of $Y(4220)$ [25]. To solve this problem, the $4S$ - $3D$ mixing scheme is introduced in Ref. [25]. It is found that when the mixing angle is around $(33 \pm 3)^\circ$, the mass of $Y(4220)$ can be reproduced, simultaneously, a partner state has mass of 4380 MeV [25]. Moreover, the study around these charmoniumlike states around 4.6 GeV also shows the important role of the S - D mixing scheme when putting them into the charmonium family [26]. So from these previous experience on constructing the charmonium family, we may find that the S - D mixing effect is universal and cannot be ignored when depicting heavy quarkonium spectroscopy.

Inspired by the research experiences of constructing the charmonium family [24–26], in this work we suggest that introducing the S - D mixing scheme can also solve the mass problem of the $\Upsilon(10753)$. Firstly, checking PDG data [1], one notices that the experimental mass of $\Upsilon(10580)$ (10579.4 MeV) is lower than the prediction of $\Upsilon(4S)$ (10607 – 10640 MeV) [19–23]. And, the mass of the newly reported $\Upsilon(10753)$ is higher than the predicted mass of $\Upsilon(3D)$ (10653 – 10717 MeV). This situation satisfies the requirement of introducing the $4S$ - $3D$ mixing, by which the mass problem of the $\Upsilon(10753)$ can be solved. In Sec. II, we will present the details of the introduced $4S$ - $3D$ mixing scheme.

It is obvious that the bottomonium assignment to the $\Upsilon(10753)$ can survive. Thus, how to distinguish these several explanations on $\Upsilon(10753)$ becomes a key point for now, which means studies on the decay behaviors of $\Upsilon(10753)$ under different assignments should be paid more attention. Till now, we notice that although there exists theoretical estimate on the corresponding open-bottom hadronic decay modes [18], the study of its hidden-bottom hadronic decays is still absent.

[§]Corresponding author

*Electronic address: liysh20@lzu.edu.cn

†Electronic address: baizy15@lzu.edu.cn

‡Electronic address: huangqi@ucas.ac.cn

¶Electronic address: xiangliu@lzu.edu.cn

This status stimulates our interest in investigating the hidden-bottom hadronic decays of $\Upsilon(10753)$ with the bottomonium assignment.

When looking at PDG [1], it is easy to find that for some hidden-bottom hadronic decays of higher bottomonia, their decay rates are anomalous [1]. For example, even for some spin flip transitions forbidden by heavy quark spin symmetry, their decay rates are still considerable [27–29]. Since these higher bottomonia mainly decay into a pair of B mesons, it is easy to estimate that coupled-channel effect may be important. Thus, as an equivalent description of the coupled-channel effect, the hadronic loop mechanism was introduced to understand the puzzling phenomena involved in hidden-bottom hadronic decays of some higher bottomonia [30–41]. For example, after introducing the contribution from the hadronic loop mechanism, the anomalous branching fractions such as $\Upsilon(10580) \rightarrow h_b(1P)\eta$ [42], $\Upsilon(10580) \rightarrow \Upsilon(nS)\pi^+\pi^-$ [43], $\Upsilon(10580) \rightarrow \Upsilon(1S)\eta$ [43], $\Upsilon(10860) \rightarrow \Upsilon(nS)\pi^+\pi^-$ [3], $\Upsilon(10860) \rightarrow h_b(nP)\pi^+\pi^-$ [44], $\Upsilon(10860, 11020) \rightarrow \pi^+\pi^-\pi^0\chi_{bJ}$ [7, 9] can be well understood [30–41]. Since $\Upsilon(10753)$ is also above the $B\bar{B}$ threshold, borrowing the former experience of studying these higher bottomonia like $\Upsilon(10580)$, $\Upsilon(10860)$ and $\Upsilon(11020)$ [30–41], the hadronic loop mechanism cannot be ignored when calculating the hidden-bottom hadronic decays of $\Upsilon(10753)$.

In this work, by taking into account the hadronic loop mechanism, we perform a study on the hidden-bottom decay channels $\Upsilon(10753) \rightarrow \Upsilon(1S)\eta^{(\prime)}$, $h_b(1P)\eta$ and $\chi_{bJ}\omega$, where the corresponding partial decay widths and branching fractions are estimated. Our results must be an important part of the physics around the newly reported $\Upsilon(10753)$, and can provide useful information to the forthcoming experiments when exploring these processes. With the joint efforts from theorists and experimentalists, we have reasons to believe that the feature of the discussed $\Upsilon(10753)$ can be understood well.

This paper is organized as follows. After the introduction, in Sec. II we introduce the $4S$ - $3D$ mixing mechanism to assign the $\Upsilon(10753)$ as a conventional bottomonium state. Then, we illustrate the detailed calculation of $\Upsilon(10753) \rightarrow \Upsilon(1S)\eta^{(\prime)}$, $h_b(1P)\eta$ and $\chi_{bJ}\omega$ in Sec. III. After that, we present numerical results in Sec. IV. Finally, the paper ends with a short summary.

II. THE $4S$ - $3D$ MIXING SCHEME

Although there exists exotic state [12–15] and kinetic effect [16, 17] interpretations to the newly observed $\Upsilon(10753)$, we still need to meticulously study the possibility that if this $\Upsilon(10753)$ can be included into the bottomonium family. In Ref. [20], a systematical investigation on the higher bottomonia was carried out by using a modified Godfrey-Isgur model¹

and predicted mass and width of the $\Upsilon(3D)$ state are 10675 MeV and 54.1 MeV, respectively.

Although the predicted width of $\Upsilon(3D)$ is consistent with the current measurement of the $\Upsilon(10753)$ [3], the predicted mass is about 70 MeV lower than the measurement. Furthermore, after checking other theoretical results on the mass spectrum of bottomonium family, we find that the predicted mass of $\Upsilon(3D)$ is in the range (10653 – 10717) MeV [19–23], which also shows that none of the predicted mass of $\Upsilon(3D)$ is close to the current measurement. In addition, after checking PDG [1], we find that the mass of $\Upsilon(10580)$ is 10579.4 MeV, which is also far away from the predicted mass (10607 – 10640) MeV [19–23].

Since the experimental masses of the $\Upsilon(10753)$ and $\Upsilon(10580)$ is higher and lower than the corresponding theoretical results, which stimulate the idea to introduce the S - D mixing mechanism, where this mixing mechanism had been successfully applied to understand the observed charmonium-like states [24–26, 48]. Especially, in Ref. [25], after introducing the $4S$ - $3D$ mixing, the mass of $Y(4220)$, whose mass is about 54 MeV lower than prediction, is reproduced well. And its partner $\psi(4380)$ was predicted, which has showed some hints in the $e^+e^- \rightarrow D\bar{D}_2^* \rightarrow D^0D^-\pi^+$, $e^+e^- \rightarrow D^0D^*\pi^+$, and $e^+e^- \rightarrow \psi(2S)\pi^+\pi^-$ processes [25].

Thus, in our view it is meaningful to investigate whether or not the introduction of $4S$ - $3D$ mixing can solve the mass problem of the $\Upsilon(10753)$. Similar to the approach in Refs. [24–26], we introduce

$$\begin{pmatrix} \Upsilon'_{4S} \\ \Upsilon'_{3D} \end{pmatrix} = \begin{pmatrix} \cos\theta & -\sin\theta \\ \sin\theta & \cos\theta \end{pmatrix} \begin{pmatrix} \Upsilon_{4S} \\ \Upsilon_{3D} \end{pmatrix}, \quad (2.1)$$

to describe the $4S$ - $3D$ mixing, where θ denotes the mixing angle. Υ_{4S} and Υ_{3D} are the wave functions of the pure $4S$ and $3D$ bottomonium states, respectively. Υ'_{4S} and Υ'_{3D} are the wave functions of the physical states, respectively.

To fix the mixing angle θ , in this work we focus on the electronic decay of bottomonium states since we already have the experimental data of $\Gamma_{ee}(\Upsilon(10580))$ [1]. The expressions we used to fit the electronic decay width are as follows [49]

$$\begin{aligned} \Gamma_{ee}(nS) &= \frac{4\alpha^2 e_b^2}{M_{nS}^2} |R_{nS}(0)|^2 \left(1 - \frac{16}{3} \frac{\alpha_s}{\pi}\right), \\ \Gamma_{ee}(nD) &= \frac{4\alpha^2 e_b^2}{M_{nD}^2} \left| \frac{5}{2\sqrt{2}m_b^2} R''_{nD}(0) \right|^2 \left(1 - \frac{16}{3} \frac{\alpha_s}{\pi}\right), \end{aligned} \quad (2.2)$$

model, the mass of $\Upsilon(3^3D_1)$ state was predicted [20]. In this work, we adopt this value as input. We noticed that there exists a systematical study of bottomonium meson family with a realistic coupled-channel calculation by considering these open-bottom meson pair channels [47], where the predicted mass of $\Upsilon(3^3D_1)$ is 10650.9 MeV, which is comparable with our adopted result 10675 MeV taken from Ref. [47]. As emphasized in Refs. [20, 47], the coupled-channel effect is obvious since the mass shift between bare mass and physical mass for $\Upsilon(3^3D_1)$ is around 90 MeV. This situation inspires us to introduce hadronic loop contribution when estimating the branching ratios of the $\Upsilon(3^3D_1)$ decays into hidden-charm decay channels in this work.

¹ As an unquenched quark model, the modified Godfrey-Isgur model is an equivalent description of the coupled-channel effect [20] since the screening potential was introduced [45, 46]. With the modified Godfrey-Isgur

where $e_b = 1/3$ is the charge of b quark, α is the fine structure constant and $\alpha_s = 0.18$ [20]. Besides, $R_{nS}(0)$ is the radial S wave function at the origin, while $R''_{nD}(0)$ is the second derivative of the radial D wave function at the origin. After considering the $4S - 3D$ mixing, the electronic decay width of the mixed $\Upsilon'(4S)$ state is

$$\Gamma_{ee} = \frac{4\alpha^2 e_b^2}{M_{\Upsilon'(4S)}^2} \left| R_{nS}(0) \cos \theta + \frac{5}{2\sqrt{2}m_b^2} R''_{nD}(0) \sin \theta \right|^2 \times \left(1 - \frac{16}{3} \frac{\alpha_s}{\pi} \right). \quad (2.3)$$

With Eq. (2.3) and the experimental data of the electronic decay width of the $\Upsilon(10580)$ ($\Gamma_{ee}(\Upsilon(10580)) = (0.272 \pm 0.029)$ KeV) [1], and after substituting into the $R_{nS}(0)$ and $R''_{nD}(0)$ extracted from Ref. [20], the mixing angle is fixed to be $\theta = (33 \pm 4)^\circ$, which is close to the results given in Refs. [22, 23].

Then, we turn to illustrate the change of mass caused by the mixing. In this mixing scheme, the mass eigenvalues of the physical states $\Upsilon'(4S)$ and $\Upsilon'(3D)$ are determined by

$$m_{\Upsilon'(4S)}^2 = \frac{1}{2} \left[m_{\Upsilon(4S)}^2 + m_{\Upsilon(3D)}^2 - \sqrt{(m_{\Upsilon(4S)}^2 - m_{\Upsilon(3D)}^2)^2 \sec^2 2\theta} \right],$$

$$m_{\Upsilon'(3D)}^2 = \frac{1}{2} \left[m_{\Upsilon(4S)}^2 + m_{\Upsilon(3D)}^2 + \sqrt{(m_{\Upsilon(4S)}^2 - m_{\Upsilon(3D)}^2)^2 \sec^2 2\theta} \right], \quad (2.4)$$

where $m_{\Upsilon(4S)}$ and $m_{\Upsilon(3D)}$ are the masses of pure $4S$ and $3D$ bottomonium states, respectively. Based on the Eq. (2.4), we investigate the θ -dependence of $m_{\Upsilon'(4S)}$ and $m_{\Upsilon'(3D)}$. As shown in Fig. 1, the mass of the physical state $\Upsilon'(4S)$ is decreased while the mass of the physical state $\Upsilon'(3D)$ is increased when increasing the mixing angle $|\theta|$. Thus, introducing the $4S-3D$ mixing scheme can reproduce the mass of the $\Upsilon(10753)$ and $\Upsilon(10580)$ well.

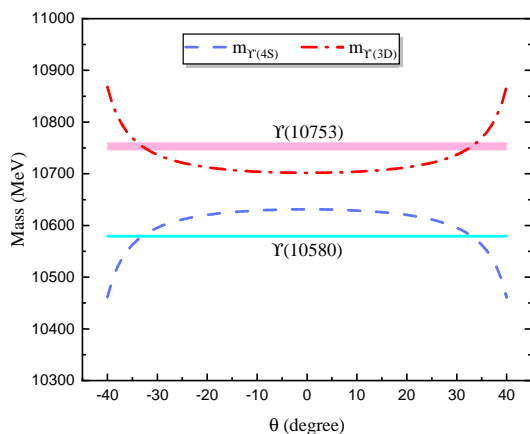


FIG. 1: The θ dependence of the masses of the physical states $\Upsilon'(4S)$ and $\Upsilon'(3D)$. Here, the cyan and pink bands denote the current measurements of $m_{\Upsilon(10580)}$ and $m_{\Upsilon(10753)}$, respectively. The masses of pure state $\Upsilon(4S)$ and $\Upsilon(3D)$ is taken as the range of (10621 – 10643) MeV and (10691 – 10712) MeV, respectively, which are from theoretical predictions [19–23].

In this section, we discuss the $S-D$ mixing scheme for $\Upsilon(10750)$ and $\Upsilon(10580)$. In fact, we have reason to believe that there should exist the mixing scheme for other pairs of quantum numbers and these mixing schemes would modify the entire spectrum. However, the present experimental information of heavy quarkonium especially for bottomonium is not enough to be applied to test such scenario. For example, F -wave charmonium states are still absent, which may have mixing with the corresponding P -wave state. For bottomonium, the $\Upsilon(1^3D_1)$ and $\Upsilon(2^3D_1)$ states are still missing in experiment. We hope that this situation can be changed with the running of Belle II. Obviously, how the mixing scheme mentioned above changes the spectroscopy behavior of heavy quarkonium is an interesting research topic not only at present but also in the future.

In general, by considering the $4S-3D$ mixing, we find a way to resolve the mass puzzle of the $\Upsilon(10580)$ and $\Upsilon(10753)$ simultaneously, where the $\Upsilon(10753)$ can be assigned as the mixture of the $4S$ and $3D$ bottomonium states. In the following, we adopt this mixing scheme to present the corresponding hidden-bottom decay behavior.

III. THE TRANSITIONS VIA THE HADRONIC LOOP MECHANISM

According to the latest Belle's result, the $\Upsilon(10753)$ is above $B^{(*)}\bar{B}^{(*)}$ and $B_s\bar{B}_s$ thresholds. Thus, the $\Upsilon(10753)$ should dominantly decay into a pair of bottomed or bottom-strange mesons. Under the framework of hadronic loop mechanism [32, 36–41], the hidden-bottom hadronic decays $\Upsilon(10753) \rightarrow \Upsilon(1S)\eta'(\prime)$, $\Upsilon(10753) \rightarrow h_b(1P)\eta$ and $\Upsilon(10753) \rightarrow \chi_{bJ}\omega$ can be achieved by the following way. Firstly, the initial $\Upsilon(10753)$ couples with $B^{(*)}\bar{B}^{(*)}$, then, the bottom meson pair converts into a low-lying bottomonia and one light meson by exchanging a $B^{(*)}$ meson. We should emphasize here that since the coupling between the $\Upsilon(10753)$ and $B_s\bar{B}_s$ is weak [18], in this work we ignore the contributions from the intermediate B_s meson loops.

According to the limits of quantum numbers and phase space, the diagrams depicting the involved decays can be determined. As discussed in Sec. II, the $\Upsilon(10753)$ can be well understood as the dressed $\Upsilon(3D)$ state with mixing the $\Upsilon(4S)$ component, so when we calculate the decay properties of the $\Upsilon(10753)$, we must consider not only the contributions from $3D$ component, but also the ones from $4S$ component. The diagrams depicting the decays to $\Upsilon(1S)\eta'(\prime)$, $h_b(1P)\eta$ and $\chi_{bJ}(1P)\omega$ are shown in Fig. 2, Fig. 3 and Fig. 4, respectively.

The general expression of the amplitude can be written as

$$\mathcal{M} = \int \frac{d^4q}{(2\pi)^4} \frac{\mathcal{V}_1 \mathcal{V}_2 \mathcal{V}_3}{\mathcal{P}_1 \mathcal{P}_2 \mathcal{P}_E} \mathcal{F}^2(q^2, m_E^2), \quad (3.1)$$

where \mathcal{V}_i ($i=1,2,3$) are interaction vertices, $1/\mathcal{P}_{1,2}$ and $1/\mathcal{P}_E$ denote the propagators of intermediate bottomed mesons. Here, $\mathcal{F}(q^2, m_E^2)$ is the form factor, which is introduced to compensate the off-shell effect of the exchanged $B^{(*)}$ meson and depict the structure effect of interaction vertices [50–52].

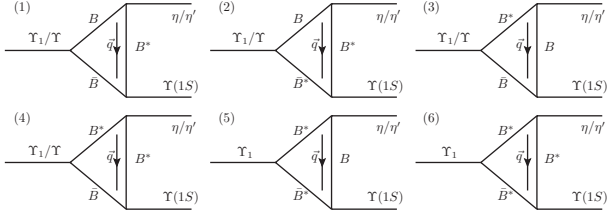


FIG. 2: The schematic diagrams for depicting the $\Upsilon(4S, 3D) \rightarrow \Upsilon(1S)\eta^{(\prime)}$ decay via the hadronic loop mechanism.

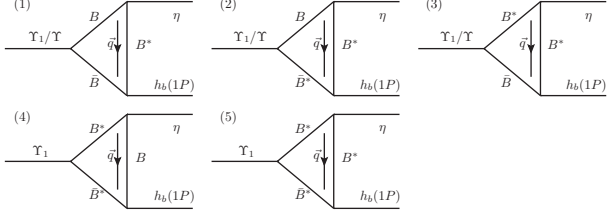


FIG. 3: The schematic diagrams for depicting the $\Upsilon(4S, 3D) \rightarrow h_b(1P)\eta$ decay via the hadronic loop mechanism.

In this paper, the monopole form factor [53] is adopted, which is written as

$$\mathcal{F}(q^2, m_E^2) = \frac{\Lambda^2 - m_E^2}{\Lambda^2 - q^2}, \quad (3.2)$$

where m_E and q denote the mass and momentum of the exchanged bottomed meson, respectively, and Λ is the cutoff, which can be parameterized as $\Lambda = m_E + \alpha_\Lambda \Lambda_{QCD}$ with $\Lambda_{QCD} = 220$ MeV [54–56] and α_Λ being a free parameter.

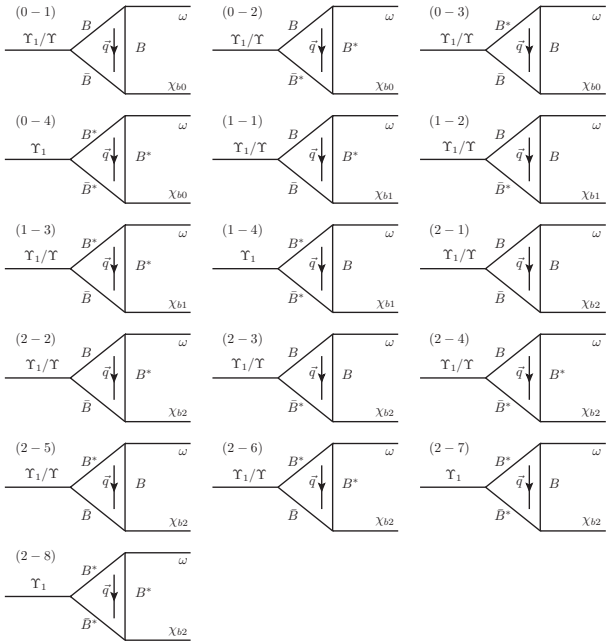


FIG. 4: The schematic diagrams for depicting the $\Upsilon(4S, 3D) \rightarrow \chi_{bJ}\omega$ ($J=0,1,2$) decay via the hadronic loop mechanism.

Usually, the free parameter α_Λ should be of order one and is dependent on the concrete processes [52].

In order to write down the amplitudes, we adopt the effective lagrangian approach to describe the involved vertices \mathcal{V}_i in Eq. (3.1). Considering the heavy quark limit and chiral symmetry, the effective Lagrangians describing the interactions involved in bottomonium, bottomed (or bottom-strange) meson pair, and light pseudoscalar (vector) meson are [57–60]

$$\begin{aligned} \mathcal{L}_S &= ig_S \text{Tr}[S^{(Q\bar{Q})} \bar{H}^{(Qq)} \gamma^\mu \overleftrightarrow{\partial}_\mu \bar{H}^{(Q\bar{q})}] + \text{H.c.}, \\ \mathcal{L}_P &= ig_P \text{Tr}[P^{(Q\bar{Q})\mu} \bar{H}^{(Qq)} \gamma^\mu \bar{H}^{(Q\bar{q})}] + \text{H.c.}, \\ \mathcal{L}_D &= ig_D \text{Tr}[D_{\mu\nu}^{(Q\bar{Q})} \bar{H}^{(Qq)} \overleftrightarrow{\partial}_\mu \gamma^\nu \bar{H}^{(Q\bar{q})}] + \text{H.c.}, \\ \mathcal{L}_\mathcal{P} &= ig_H \text{Tr}[H^{(Q\bar{q})j} \gamma_\mu \gamma_5 (\mathcal{A}^\mu)^i \bar{H}_i^{(Qq)}], \\ \mathcal{L}_\mathcal{V} &= i\beta \text{Tr}[H^{(Q\bar{q})j} \nu^\mu (-\rho_\mu)_j^i \bar{H}_i^{(Qq)}] \\ &\quad + i\lambda \text{Tr}[H^{(Q\bar{q})j} \sigma^{\mu\nu} F_{\mu\nu} (\rho_j^i) \bar{H}_i^{(Qq)}] \end{aligned} \quad (3.3)$$

with $\overleftrightarrow{\partial} = \overrightarrow{\partial} - \overleftarrow{\partial}$. In Eq. (3.3), $S^{(Q\bar{Q})}$, $P^{(Q\bar{Q})\mu}$ and $D_{\mu\nu}^{(Q\bar{Q})}$ denote the S -wave, P -wave and D -wave multiplets of bottomonium, respectively. $H^{(Q\bar{q})}$ and $\bar{H}^{(Qq)}$ are $(0^-, 1^-)$ doublets of bottom and anti-bottom mesons respectively. \mathcal{A}^μ is the axial vector current of Nambu-Goldstone fields, which reads as $\mathcal{A}^\mu = (\xi^\dagger \partial^\mu \xi - \xi \partial^\mu \xi^\dagger)/2$ with $\xi = e^{i\mathbb{P}/f_\pi}$. In addition, $\rho_\mu = ig_V \nabla_\mu / \sqrt{2}$ and $F_{\mu\nu}(\rho) = \partial_\mu \rho_\nu - \partial_\nu \rho_\mu + [\rho_\mu, \rho_\nu]$ [38, 61–63]. For the detailed expressions of these symbols, we collect them into Appendix A.

After expanding the above Lagrangians, the concerned effective Lagrangians, as shown in Appendix A, can be obtained. Thus, we can write down the concrete amplitudes corresponding to the diagrams in Figs. 2–4. For example, with the Feynman rules listed in Appendix B, the amplitude of the first diagram in Fig. 2 can be obtained as

$$\begin{aligned} \mathcal{M}_{3D}^{(1)} &= i^3 \int \frac{d^4 q}{(2\pi)^4} g_{\Upsilon_1 BB} \epsilon_{\Upsilon_1}^\lambda \epsilon_{\Upsilon_1}^{\nu*} (q_{1\lambda} - q_{2\lambda}) g_{\Upsilon BB^*} \epsilon_{\mu\nu\alpha\beta} \\ &\quad \times p_2^\mu (q_2^\beta - q^\beta) g_{BB^* \eta^{(\prime)}} p_1^\tau \frac{1}{q_1^2 - m_B^2} \frac{1}{q_2^2 - m_B^2} \\ &\quad \times \frac{-g_\tau^\alpha + q_\tau q^\alpha / m_{B^*}^2}{q^2 - m_{B^*}^2} \mathcal{F}^2(q^2, m_{B^*}^2). \end{aligned} \quad (3.4)$$

And then, the remaining amplitudes can be written down similarly.

Finally, the decay widths of the transitions of the $\Upsilon(10753)$ into a low-lying bottomonium by emitting a light pseudoscalar meson $\eta^{(\prime)}$ or ω can be evaluated by

$$\Gamma = \frac{1}{3} \frac{|\vec{p}|}{8\pi m^2} |\overline{\mathcal{M}^{\text{Total}}}|^2, \quad (3.5)$$

where the overbar denotes to sum over the polarizations of $\Upsilon(1S)$, $h_b(1P)$ or $\chi_{bJ}(1P)$ ($J=0,1,2$), and the vector meson ω . The coefficient $1/3$ comes from averaging over polarizations of the initial state. \vec{p} is the momentum of the light meson. The general expression of total amplitudes is

$$\mathcal{M}^{\text{Total}} = 4 \sum_{i=1}^{i_{\max}} \mathcal{M}_{4S}^{(i)} \sin \theta + 4 \sum_{j=1}^{j_{\max}} \mathcal{M}_{3D}^{(j)} \cos \theta. \quad (3.6)$$

Here, the superscript $i(j)$ denotes the $i(j)$ -th amplitudes from bottomed meson loops in the above diagrams, while the subscripts $4S$ and $3D$ denote the contributions from $\Upsilon(4S)$ or $\Upsilon(3D)$ components, respectively, $\theta = 33^\circ$ is used in this work. In addition, the factor 4 comes from the charge conjugation and the isospin transformations on the bridged $B^{(*)}$ meson.

IV. NUMERICAL RESULTS

Before presenting the numerical results, we need to illustrate how to determine the relevant coupling constants. The coupling constants $g_{\Upsilon, B^{(*)}B^{(*)}}$ depicting the coupling between $\Upsilon(3D)$ and a pair of bottomed mesons are extracted from the corresponding decays widths, which are quoted from Ref. [20]. The decay widths and the corresponding coupling constants are listed in Table I. As for $g_{\Upsilon(4S)BB^{(*)}}$, the $g_{\Upsilon(4S)BB}$ is determined by the corresponding partial decay width given in Ref. [20], while the $g_{\Upsilon(4S)BB^*}$ can be fixed by $g_{\Upsilon(4S)BB}$ and Eq. (4.1) in heavy quark symmetry. Numerically, $g_{\Upsilon(4S)BB} = 13.224$ and $g_{\Upsilon(4S)BB^*} = 1.251 \text{ GeV}^{-1}$ are used in this work.

TABLE I: The decay widths of $\Upsilon(3D) \rightarrow B^{(*)}\bar{B}^{(*)}$ given in Ref. [20] and the extracted coupling constants $g_{\Upsilon, B^{(*)}B^{(*)}}$ of $\Upsilon(3D)$ coupling with $B^{(*)}\bar{B}^{(*)}$.

Channel	Decay width (MeV)	Coupling constant
BB	5.47	3.480
$B\bar{B}^* + \text{c.c.}$	15.2	0.393 GeV^{-1}
$B^*\bar{B}^*$	33.4	4.210

For $g_{\Upsilon B^{(*)}B^{(*)}}$, $g_{h_b B^{(*)}B^{(*)}}$ and $g_{\chi_{b1} B^{(*)}B^{(*)}}$ defined in Eq. (1.8), Eq. (1.9) and Eq. (1.10), respectively, the symmetry implied by the heavy quark effective theory is needed to be considered. Under this symmetry, these coupling constants are related to each others through the global constants g_S and g_P , which are expressed as

$$\begin{aligned}
\frac{g_{\Upsilon BB}}{m_B} &= \frac{g_{\Upsilon BB^*} m_{\Upsilon}}{\sqrt{m_B m_{B^*}}} = \frac{g_{\Upsilon B^* B^*}}{m_{B^*}} = 2g_S \sqrt{m_{\Upsilon}}, \\
\frac{g_{h_b BB^*}}{\sqrt{m_B m_{B^*}}} &= g_{h_b B^* B^*} \frac{m_{h_b}}{m_{B^*}} = 2g_P \sqrt{m_{h_b}}, \\
\frac{g_{\chi_{b0} BB}}{\sqrt{3} m_B} &= \frac{\sqrt{3} g_{\chi_{b0} B^* B^*}}{m_{B^*}} = 2\sqrt{m_{\chi_{b0}}} g_P, \\
g_{\chi_{b1} BB^*} &= 2\sqrt{2} \sqrt{m_B m_{B^*} m_{\chi_{b1}}} g_P, \\
g_{\chi_{b2} BB m_B} &= g_{\chi_{b2} BB^*} \sqrt{m_B m_{B^*} m_{\chi_{b2}}} = \frac{g_{\chi_{b2} B^* B^*}}{4m_{B^*}} = \sqrt{m_{\chi_{b2}}} g_P,
\end{aligned} \tag{4.1}$$

where $g_S = 0.407 \text{ GeV}^{-3/2}$ [41], and $g_P = -\sqrt{\frac{m_{\chi_{b0}}}{3}} \frac{1}{f_{\chi_{b0}}}$ with $f_{\chi_{b0}} = 175 \pm 55 \text{ MeV}$ is obtained by QCD sum rule [64].

Additionally, $g_{B^{(*)}B^{(*)}\eta}$ can be expressed by the coupling con-

stant g_H , i.e.,

$$\begin{aligned}
\frac{g_{BB^*\eta}}{\sqrt{m_B m_{B^*}}} &= g_{B^* B^* \eta} = \frac{2g_H}{f_\pi} \alpha, \\
\frac{g_{BB^*\eta'}}{\sqrt{m_B m_{B^*}}} &= g_{B^* B^* \eta'} = \frac{2g_H}{f_\pi} \beta,
\end{aligned} \tag{4.2}$$

where $g_H = 0.569$, $f_\pi = 131 \text{ MeV}$ [37, 40, 41], α and β were defined in Eq. (1.6). And $g_{B^{(*)}B^{(*)}\omega}$ is related to the global coupling constant g_V , i.e.,

$$\begin{aligned}
g_{BB\omega} &= g_{B^* B^* \omega} = \frac{\beta g_V}{2}, \\
f_{BB^*\omega} &= \frac{f_{B^* B^* \omega}}{m_{B^*}} = \frac{\lambda g_V}{2},
\end{aligned} \tag{4.3}$$

where $\beta = 0.9$, $\lambda = 0.56 \text{ GeV}^{-1}$, and $g_V = m_\rho/f_\pi$ [38].

A. The result of processes with $\eta^{(\prime)}$ emission

In this subsection, we present our results of the $\Upsilon(10753) \rightarrow \Upsilon(1S)\eta^{(\prime)}$, $\Upsilon(10753) \rightarrow h_b(1P)\eta$ processes. Apart from the fixed coupling constants, there still exists a free parameter α_Λ , which comes from the introduced form factor. Following Ref. [37–40], in this work we still set $0.5 \leq \alpha_\Lambda \leq 1.0$ to calculate the decay widths and the corresponding branching fractions for the $\Upsilon(10753) \rightarrow \Upsilon(1S)\eta^{(\prime)}$ and $\Upsilon(10753) \rightarrow h_b(1P)\eta$ processes, and the numerical results are shown in Fig. 5.

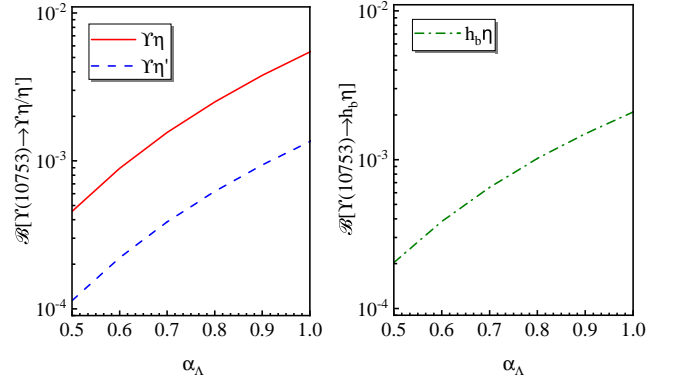


FIG. 5: The α_Λ dependence of the branching fractions $\mathcal{B}[\Upsilon(10753) \rightarrow \Upsilon(1S)\eta^{(\prime)}]$ (left panel) and $\mathcal{B}[\Upsilon(10753) \rightarrow h_b(1P)\eta]$ (right panel).

Thus, the decay widths of $\Upsilon(10753) \rightarrow \Upsilon(1S)\eta^{(\prime)}$, $\Upsilon(10753) \rightarrow h_b(1P)\eta$ processes are

$$\begin{aligned}
\Gamma[\Upsilon(10753) \rightarrow \Upsilon(1S)\eta] &= (16.2 - 193.7) \text{ keV}, \\
\Gamma[\Upsilon(10753) \rightarrow \Upsilon(1S)\eta'] &= (4.04 - 48.0) \text{ keV}, \\
\Gamma[\Upsilon(10753) \rightarrow h_b(1P)\eta] &= (7.23 - 74.2) \text{ keV},
\end{aligned}$$

which are transferred from these branching fractions

$$\mathcal{B}[\Upsilon(10753) \rightarrow \Upsilon(1S)\eta] = (0.46 - 5.46) \times 10^{-3},$$

$$\begin{aligned}\mathcal{B}[\Upsilon(10753) \rightarrow \Upsilon(1S)\eta'] &= (0.11 - 1.35) \times 10^{-3}, \\ \mathcal{B}[\Upsilon(10753) \rightarrow h_b(1P)\eta] &= (0.20 - 2.09) \times 10^{-3}.\end{aligned}$$

Our results show that the branching fractions of the $\Upsilon(10753) \rightarrow \Upsilon(1S)\eta$, $\Upsilon(10753) \rightarrow h_b(1P)\eta$ processes can reach up to 10^{-3} , and the branching ratio of $\Upsilon(10753) \rightarrow \Upsilon(1S)\eta'$ is around 10^{-4} , which indicates that these discussed transitions can be accessible at the Belle II experiment. In addition, we provide the ratio $R_{\eta'/\eta} = \mathcal{B}[\Upsilon(10753) \rightarrow \Upsilon(1S)\eta']/\mathcal{B}[\Upsilon(10753) \rightarrow \Upsilon(1S)\eta]$ as

$$R_{\eta'/\eta} \approx 0.25,$$

which is weakly dependent on the cutoff parameter α_Λ . The behavior of $R_{\eta'/\eta}$ can be further tested in future experiments.

B. The result of the processes with ω emission

Next, we investigate the hadronic loop contribution to the $\Upsilon(10753) \rightarrow \chi_{bj}\omega$ ($J = 0, 1, 2$) decays, where the α_Λ dependence of branching fractions are shown in Fig. 6.

From Fig. 6 we can get that the corresponding branching fractions are

$$\begin{aligned}\mathcal{B}[\Upsilon(10753) \rightarrow \chi_{b0}\omega] &= (0.73 - 6.94) \times 10^{-3}, \\ \mathcal{B}[\Upsilon(10753) \rightarrow \chi_{b1}\omega] &= (0.25 - 2.16) \times 10^{-3}, \\ \mathcal{B}[\Upsilon(10753) \rightarrow \chi_{b2}\omega] &= (1.08 - 11.5) \times 10^{-3}.\end{aligned}$$

Thus the corresponding decay widths are

$$\begin{aligned}\Gamma[\Upsilon(10753) \rightarrow \chi_{b0}\omega] &= (25.9 - 246.5) \text{ keV}, \\ \Gamma[\Upsilon(10753) \rightarrow \chi_{b1}\omega] &= (8.79 - 76.8) \text{ keV}, \\ \Gamma[\Upsilon(10753) \rightarrow \chi_{b2}\omega] &= (38.2 - 407.7) \text{ keV}.\end{aligned}$$

Additionally, we also notice that the behavior of the ratios $R_{ij} = \mathcal{B}[\Upsilon(10753) \rightarrow \chi_{bi}\omega]/\mathcal{B}[\Upsilon(10753) \rightarrow \chi_{bj}\omega]$ (see Fig. 6) are also weakly dependent on the parameter α_Λ , i.e.,

$$\begin{aligned}R_{10} &= \frac{\mathcal{B}[\Upsilon(10753) \rightarrow \chi_{b1}\omega]}{\mathcal{B}[\Upsilon(10753) \rightarrow \chi_{b0}\omega]} = (0.33 - 0.35), \\ R_{12} &= \frac{\mathcal{B}[\Upsilon(10753) \rightarrow \chi_{b1}\omega]}{\mathcal{B}[\Upsilon(10753) \rightarrow \chi_{b2}\omega]} = (0.18 - 0.22), \\ R_{02} &= \frac{\mathcal{B}[\Upsilon(10753) \rightarrow \chi_{b0}\omega]}{\mathcal{B}[\Upsilon(10753) \rightarrow \chi_{b2}\omega]} = (0.55 - 0.63).\end{aligned}$$

Obviously, experimental measurement for them will be an interesting issue for future experiments such as Belle II.

V. SUMMARY

Recently, the Belle Collaboration released a new analysis on the $e^+e^- \rightarrow \Upsilon(nS)\pi^+\pi^-$ processes ($n = 1, 2, 3$) and found the evidence of a new structure near 10.75 GeV [3], whose mass and width are fitted as $M = (10752.7 \pm 5.9_{-1.1}^{+0.7})$ MeV and $\Gamma = (35.5_{-11.3-3.3}^{+17.6+3.9})$ MeV, respectively. Although the width of this state is consistent with the prediction of $\Upsilon(3D)$ given by

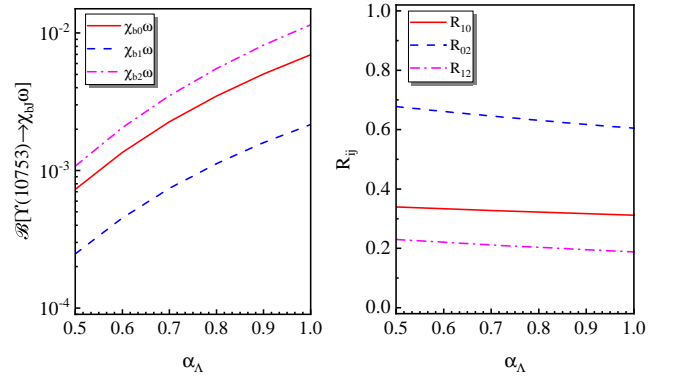


FIG. 6: The α_Λ dependence of the branching fractions $\mathcal{B}[\Upsilon(10753) \rightarrow \chi_{bj}\omega]$ (left panel) and the α_Λ dependence of the ratios $R_{ij} = \mathcal{B}[\Upsilon(10753) \rightarrow \chi_{bi}\omega]/\mathcal{B}[\Upsilon(10753) \rightarrow \chi_{bj}\omega]$ (right panel).

Ref. [20], its mass can not match any of the previous theoretical results of $\Upsilon(3D)$ [19–23].

To solve the mass problem of this $\Upsilon(10753)$, based on the experience on the charmonium family [24–26, 48], $4S - 3D$ mixing is introduced. It is found that when the mixing angle is around $(33 \pm 4)^\circ$, the masses of the $\Upsilon(10580)$ and $\Upsilon(10753)$ can be reproduced simultaneously. Besides, the obtained masses of pure $4S$ and $3D$ states are consistent with [19–23]. Thus, in our view, the newly observed $\Upsilon(10753)$ can be assigned as a bottomonium state with $4S-3D$ mixing.

To further understand the nature of this $\Upsilon(10753)$, study on its decay behavior is necessary. Since the study of its hidden-bottom hadronic decays is still absent, in this work we carry out a study on some hidden-bottom decays of the $\Upsilon(10753)$, which include $\Upsilon(10753) \rightarrow \Upsilon(1S)\eta^{(\prime)}$, $\Upsilon(10753) \rightarrow h_b(1P)\eta$ and $\Upsilon(10753) \rightarrow \chi_{bj}\omega$ ($J=0,1,2$).

Due to the typical feature that the $\Upsilon(10753)$ has the mass above the $B\bar{B}$ threshold, the coupled-channel effect should be considered, thus in this work we absorb the hadronic loop mechanism into the realistic study on the $\Upsilon(10753)$. We obtain the partial decay widths and the corresponding branching fractions of these discussed hidden-bottom decays, which show that $\Upsilon(10753) \rightarrow \Upsilon(1S)\eta^{(\prime)}$, $\Upsilon(10753) \rightarrow h_b(1P)\eta$ and $\Upsilon(10753) \rightarrow \chi_{bj}\omega$ ($J=0,1,2$) have considerable decay rates, which we think are accessible in future experiments such as Belle II. Furthermore, we obtain some typical values which are almost independent the free parameter introduced by the form factor, which can be important values for us to study the decay behavior of this $\Upsilon(10753)$ and understand its nature.

In conclusion, it is obvious that future experimental search for these discussed hidden-bottom hadronic decays of the $\Upsilon(10753)$ will be an intriguing task, by which the nature of the $\Upsilon(10753)$ should be decoded. Thus, We strongly encourage the running Belle II experiment to pay attention to this issue.

ACKNOWLEDGMENTS

This work is supported by the China National Funds for Distinguished Young Scientists under Grant No. 11825503, National Key Research and Development Program of China under Contract No. 2020YFA0406400, and the 111 Project under Grant No. B20063, the National Natural Science Foundation of China under Grant No. 12047501.

Appendix A

In this appendix, we give the adopted Lagrangians in detail. The $S^{(Q\bar{Q})}$, $P^{(Q\bar{Q})\mu}$ and $D^{(Q\bar{Q})\mu\nu}$ denote the S -wave, P -wave and D -wave multiplets of the bottomonia with expressions

$$S^{(Q\bar{Q})} = \frac{1+\psi}{2} [\Upsilon^\mu \gamma_\mu - \eta_b \gamma_5] \frac{1-\psi}{2}, \quad (1.1)$$

$$P^{(Q\bar{Q})\mu} = \frac{1+\psi}{2} \left[\chi_{b2}^{\mu\alpha} \gamma_\alpha + \frac{1}{\sqrt{2}} \varepsilon^{\mu\alpha\beta\gamma} \nu_\alpha \gamma_\beta \chi_{b1\gamma} + \frac{1}{\sqrt{3}} (\gamma^\mu - \nu^\mu) \chi_{b0} + h_b^\mu \gamma_5 \right] \frac{1-\psi}{2}, \quad (1.2)$$

$$D^{(Q\bar{Q})\mu\nu} = \frac{1+\psi}{2} \left[\Upsilon_3^{\mu\nu\alpha} \gamma_\alpha + \frac{1}{\sqrt{6}} (\varepsilon^{\mu\alpha\beta\rho} \nu_\alpha \gamma_\beta \Upsilon_{2\rho}^\nu + \varepsilon^{\nu\alpha\beta\rho} \nu_\alpha \gamma_\beta \times \Upsilon_{2\rho}^\mu) + \frac{\sqrt{15}}{10} [(\gamma^\mu - \nu^\mu) \Upsilon_1^\nu + (\gamma^\nu - \nu^\nu) \Upsilon_1^\mu] - \frac{1}{\sqrt{15}} (g^{\mu\nu} - \nu^\mu \nu^\nu) \gamma_\alpha \Upsilon_1^\alpha + \eta_{b2}^{\mu\nu} \gamma_5 \right] \frac{1-\psi}{2}, \quad (1.3)$$

respectively. $H^{(Q\bar{q})}$ represents the spin doublet of bottom meson filed $(\mathcal{B}, \mathcal{B}^*)$ and $H^{(\bar{Q}q)}$ corresponds to the anti-meson counterpart. Their concrete expressions are [58, 59]

$$H^{(Q\bar{q})} = \frac{1+\psi}{2} (\mathcal{B}^{*\mu} \gamma_\mu + i\mathcal{B} \gamma_5), \quad (1.4)$$

$$H^{(\bar{Q}q)} = (\bar{\mathcal{B}}^{*\mu} \gamma_\mu + i\bar{\mathcal{B}} \gamma_5) \frac{1-\psi}{2}$$

with $\bar{H}^{(Q\bar{q})} = \gamma_0 H^{(Q\bar{q})} \gamma_0$ and $\bar{H}^{(\bar{Q}q)} = \gamma_0 H^{(\bar{Q}q)} \gamma_0$.

In addition, the pseudoscalar octet \mathbb{P} reads as

$$\mathbb{P} = \begin{pmatrix} \frac{\pi^0}{\sqrt{2}} + \alpha\eta + \beta\eta' & \pi^+ & K^+ \\ \pi^- & -\frac{\pi^0}{\sqrt{2}} + \alpha\eta + \beta\eta' & K^0 \\ K^- & \bar{K}^0 & \gamma\eta + \delta\eta' \end{pmatrix} \quad (1.5)$$

with

$$\alpha = \frac{\cos\theta - \sqrt{2}\sin\theta}{\sqrt{6}}, \quad \beta = \frac{\sin\theta + \sqrt{2}\cos\theta}{\sqrt{6}}, \quad (1.6)$$

$$\gamma = \frac{-2\cos\theta - \sqrt{2}\sin\theta}{\sqrt{6}}, \quad \delta = \frac{-2\sin\theta + \sqrt{2}\cos\theta}{\sqrt{6}},$$

and the mixing angle $\theta = -19.1^\circ$ [37, 41, 65, 66], while the expression of \mathbb{V} reads as

$$\mathbb{V} = \begin{pmatrix} \frac{1}{\sqrt{2}}(\rho^0 + \omega) & \rho^+ & K^{*+} \\ \rho^- & \frac{1}{\sqrt{2}}(-\rho^0 + \omega) & K^{*0} \\ K^{*-} & \bar{K}^{*0} & \phi \end{pmatrix}. \quad (1.7)$$

With the above preparation, the compact Lagrangians in Eq. (3.3) can be expanded as

$$\begin{aligned} \mathcal{L}_{\Upsilon\mathcal{B}^{(*)}\mathcal{B}^{(*)}} &= ig_{\Upsilon\mathcal{B}\mathcal{B}} \Upsilon^\mu (\partial_\mu \mathcal{B}^\dagger \mathcal{B} - \mathcal{B}^\dagger \partial_\mu \mathcal{B}) \\ &+ g_{\Upsilon\mathcal{B}\mathcal{B}^*} \varepsilon_{\mu\nu\alpha\beta} \partial^\mu \Upsilon^\nu (\mathcal{B}^{*\alpha} \partial^\beta \mathcal{B}^\dagger - \mathcal{B} \partial^\beta \mathcal{B}^{*\alpha\dagger}) \\ &+ ig_{\Upsilon\mathcal{B}^*\mathcal{B}^*} \Upsilon^\mu (\mathcal{B}^{*\nu} \partial_\nu \mathcal{B}_\mu^{*\dagger} - \mathcal{B}^{*\dagger\nu} \partial_\nu \mathcal{B}_\mu^* - \mathcal{B}^{*\nu} \partial_\mu \mathcal{B}_\nu^{*\dagger}), \end{aligned} \quad (1.8)$$

$$\begin{aligned} \mathcal{L}_{h_b\mathcal{B}^{(*)}\mathcal{B}^{(*)}} &= -g_{h_b\mathcal{B}\mathcal{B}^*} (\mathcal{B}^\dagger \mathcal{B}_\mu^* + \mathcal{B}_\mu^{*\dagger} \mathcal{B}) h_b^\mu \\ &- ig_{h_b\mathcal{B}^*\mathcal{B}^*} \varepsilon_{\alpha\beta\mu\nu} \mathcal{B}^{*\alpha} \mathcal{B}^{*\dagger\beta} \partial^\nu h_b^\mu, \end{aligned} \quad (1.9)$$

$$\begin{aligned} \mathcal{L}_{\chi_{b0}\mathcal{B}^{(*)}\mathcal{B}^{(*)}} &= ig_{\chi_{b0}\mathcal{B}\mathcal{B}} \chi_{b0} \mathcal{B} \mathcal{B}^\dagger - ig_{\chi_{b0}\mathcal{B}^*\mathcal{B}^*} \chi_{b0} \mathcal{B}^{*\mu} \mathcal{B}_\mu^{*\dagger} \\ &- ig_{\chi_{b1}\mathcal{B}\mathcal{B}^*} \chi_{b1}^\mu (\mathcal{B}_\mu^* \mathcal{B}^\dagger - \mathcal{B} \mathcal{B}_\mu^{*\dagger}) \\ &+ ig_{\chi_{b2}\mathcal{B}\mathcal{B}} \chi_{b2}^{\mu\nu} \partial_\mu \mathcal{B} \partial_\nu \mathcal{B}^\dagger + ig_{\chi_{b2}\mathcal{B}^*\mathcal{B}^*} \chi_{b2}^{\mu\nu} \mathcal{B}_\mu^* \mathcal{B}_\nu^{*\dagger} \\ &+ g_{\chi_{b2}\mathcal{B}^*\mathcal{B}^*} \varepsilon_{\mu\nu\alpha\beta} \partial^\alpha \chi_{b2}^{\mu\rho} (\partial_\rho \mathcal{B}^{*\beta} \partial^\beta \mathcal{B}^\dagger - \partial^\beta \mathcal{B} \partial_\rho \mathcal{B}^{*\dagger\nu}), \end{aligned} \quad (1.10)$$

$$\begin{aligned} \mathcal{L}_{\Upsilon_1\mathcal{B}^{(*)}\mathcal{B}^{(*)}} &= ig_{\Upsilon_1\mathcal{B}\mathcal{B}} \Upsilon_1^\mu (\partial_\mu \mathcal{B}^\dagger \mathcal{B} - \mathcal{B}^\dagger \partial_\mu \mathcal{B}) \\ &- g_{\Upsilon_1\mathcal{B}\mathcal{B}^*} \varepsilon_{\mu\nu\alpha\beta} \partial^\nu \Upsilon_1^\alpha (\mathcal{B}^{*\beta} \partial^\mu \mathcal{B}^\dagger - \mathcal{B} \partial^\mu \mathcal{B}^{*\beta\dagger}) \\ &+ ig_{\Upsilon_1\mathcal{B}^*\mathcal{B}^*} \Upsilon_1^\mu (-4\mathcal{B}^{*\nu} \partial_\mu \mathcal{B}_\nu^{*\dagger} + \mathcal{B}^{*\nu} \partial_\nu \mathcal{B}_\mu^{*\dagger} \\ &- \mathcal{B}^{*\nu\dagger} \partial_\nu \mathcal{B}_\mu^*), \end{aligned} \quad (1.11)$$

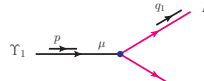
$$\begin{aligned} \mathcal{L}_{\mathcal{B}^{(*)}\mathcal{B}^{(*)}\mathbb{P}} &= ig_{\mathcal{B}\mathcal{B}\mathbb{P}} (\mathcal{B}_\mu^{*\dagger} \mathcal{B} - \mathcal{B}^\dagger \mathcal{B}_\mu^*) \partial^\mu \mathbb{P} \\ &- g_{\mathcal{B}^*\mathcal{B}^*\mathbb{P}} \varepsilon_{\mu\nu\alpha\beta} \partial^\mu \mathcal{B}^{*\dagger\nu} \partial^\alpha \mathcal{B}^{*\beta} \mathbb{P}, \end{aligned} \quad (1.12)$$

$$\begin{aligned} \mathcal{L}_{\mathcal{B}^{(*)}\mathcal{B}^{(*)}\mathbb{V}} &= -ig_{\mathcal{B}\mathcal{B}\mathbb{V}} \mathcal{B}_i^{*\dagger} \partial^i \mathcal{B}^j (\mathbb{V}_\mu)_j^\dagger \\ &- 2f_{\mathcal{B}^*\mathcal{B}^*\mathbb{V}} \varepsilon_{\mu\nu\alpha\beta} \partial^\mu (\mathbb{V}_\nu)_j^\dagger (\mathcal{B}_i^{*\dagger} \partial^\alpha \mathcal{B}^{*\beta j} - \mathcal{B}_i^{*\beta\dagger} \partial^\alpha \mathcal{B}^j) \\ &+ ig_{\mathcal{B}^*\mathcal{B}^*\mathbb{V}} \mathcal{B}_i^{*\nu\dagger} \partial^i \mathcal{B}_\nu^{*j} (\mathbb{V}_\mu)_j^\dagger \\ &+ 4if_{\mathcal{B}^*\mathcal{B}^*\mathbb{V}} \mathcal{B}_i^{*\mu\dagger} (\partial_\mu \mathbb{V}_\nu - \partial_\nu \mathbb{V}_\mu)_j^\dagger \mathcal{B}^{*\nu j}, \end{aligned} \quad (1.13)$$

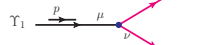
where $\mathcal{B}^{(*)\dagger}$ and $\mathcal{B}^{(*)}$ are defined as $\mathcal{B}^{(*)\dagger} = (\mathcal{B}^{(*)+}, \mathcal{B}^{(*)0}, \mathcal{B}_s^{(*)0})$ and $\mathcal{B}^{(*)} = (\mathcal{B}^{(*)-}, \bar{\mathcal{B}}^{(*)0}, \bar{\mathcal{B}}_s^{(*)0})^T$, respectively.

Appendix B

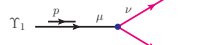
In this appendix, the Feynman rules for each interaction vertex involved in our calculation are collected. We list the concrete information as follows



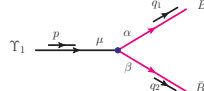
$$\Upsilon_1 \equiv -g_{\Upsilon_1 BB} \epsilon_{\Upsilon_1}^{\mu} (q_{1\mu} - q_{2\mu}), \quad (2.1)$$



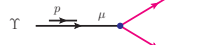
$$\Upsilon_1 \equiv g_{\Upsilon_1 BB^*} \epsilon_{\alpha\beta\mu\nu} \epsilon_{\Upsilon_1}^{\mu} p^{\beta} (q_2^{\alpha} - q_1^{\alpha}) \epsilon_{B^*}^{*\nu}, \quad (2.2)$$



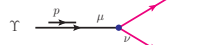
$$\Upsilon_1 \equiv g_{\Upsilon_1 BB^*} \epsilon_{\alpha\beta\mu\nu} \epsilon_{\Upsilon_1}^{\mu} p^{\beta} (q_1^{\alpha} - q_2^{\alpha}) \epsilon_{B^*}^{*\nu}, \quad (2.3)$$



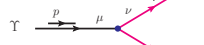
$$\Upsilon_1 \equiv -g_{\Upsilon_1 B^* B^*} \epsilon_{\Upsilon_1}^{\mu} (-4g_{\alpha\beta} (q_{1\mu} - q_{2\mu}) + g_{\alpha\mu} q_{1\beta} - g_{\beta\mu} q_{2\alpha}) \epsilon_{B^*}^{*\alpha} \epsilon_{B^*}^{*\beta}, \quad (2.4)$$



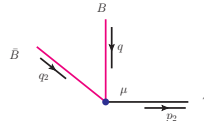
$$\Upsilon \equiv -g_{\Upsilon BB} \epsilon_{\Upsilon}^{\mu} (q_{1\mu} - q_{2\mu}), \quad (2.5)$$



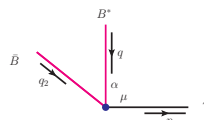
$$\Upsilon \equiv g_{\Upsilon BB^*} \epsilon_{\alpha\beta\mu\nu} \epsilon_{\Upsilon}^{\mu} p^{\beta} (q_2^{\alpha} - q_1^{\alpha}) \epsilon_{B^*}^{*\nu}, \quad (2.6)$$



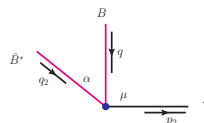
$$\Upsilon \equiv g_{\Upsilon BB^*} \epsilon_{\alpha\beta\mu\nu} \epsilon_{\Upsilon}^{\mu} p^{\beta} (q_1^{\alpha} - q_2^{\alpha}) \epsilon_{B^*}^{*\nu}, \quad (2.7)$$



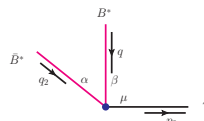
$$\bar{B} \equiv g_{\Upsilon BB} \epsilon_{\Upsilon}^{*\mu} (q_{2\mu} - q_{\mu}), \quad (2.8)$$



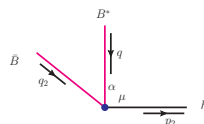
$$\bar{B} \equiv g_{\Upsilon BB^*} \epsilon_{\mu\nu\alpha\beta} \epsilon_{\Upsilon}^{*\mu} p_2^{\nu} (q^{\beta} - q_2^{\beta}) \epsilon_{B^*}^{\alpha}, \quad (2.9)$$



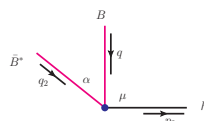
$$\bar{B}^* \equiv g_{\Upsilon BB^*} \epsilon_{\mu\nu\alpha\beta} \epsilon_{\Upsilon}^{*\mu} p_2^{\nu} (q_2^{\beta} - q^{\beta}) \epsilon_{B^*}^{\alpha}, \quad (2.10)$$



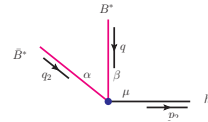
$$\bar{B}^* \equiv g_{\Upsilon B^* B^*} \epsilon_{\Upsilon}^{*\mu} (g_{\alpha\mu} q_{2\beta} - g_{\beta\mu} q_{\alpha} - g_{\alpha\beta} q_{2\mu} + g_{\alpha\beta} q_{\mu}) \epsilon_{B^*}^{\alpha} \epsilon_{B^*}^{\beta}, \quad (2.11)$$



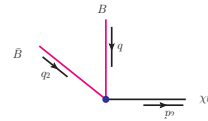
$$\bar{B} \equiv -g_{h_b BB^*} \epsilon_{h_b}^{*\mu} \epsilon_{B^*}^{\alpha} g_{\mu\alpha}, \quad (2.12)$$



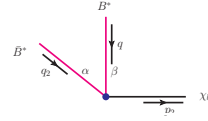
$$\bar{B}^* \equiv -g_{h_b BB^*} \epsilon_{h_b}^{*\mu} \epsilon_{B^*}^{\alpha} g_{\mu\alpha}, \quad (2.13)$$



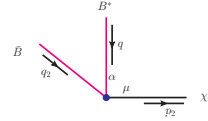
$$\bar{B}^* \equiv g_{h_b B^* B^*} \epsilon_{\beta\alpha\mu\nu} \epsilon_{h_b}^{*\mu} p_2^{\nu} \epsilon_{B^*}^{\alpha} \epsilon_{B^*}^{\beta}, \quad (2.14)$$



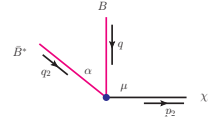
$$\bar{B} \equiv i g_{\chi_{b0} BB}, \quad (2.15)$$



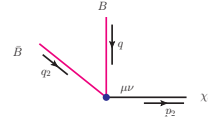
$$\bar{B}^* \equiv -i g_{\chi_{b0} B^* B^*} \epsilon_{B^*}^{\alpha} \epsilon_{B^*}^{\beta} g_{\alpha\beta}, \quad (2.16)$$



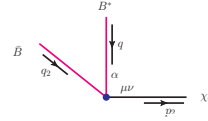
$$\bar{B} \equiv -i g_{\chi_{b1} BB^*} \epsilon_{\chi_{b1}}^{*\mu} \epsilon_{B^*}^{\alpha} g_{\mu\alpha}, \quad (2.17)$$



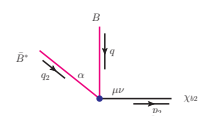
$$\bar{B}^* \equiv i g_{\chi_{b1} BB^*} \epsilon_{\chi_{b1}}^{*\mu} \epsilon_{B^*}^{\alpha} g_{\mu\alpha}, \quad (2.18)$$



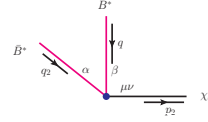
$$\bar{B} \equiv -i g_{\chi_{b2} BB} \epsilon_{\chi_{b2}}^{*\mu\nu} q_{\mu} q_{2\nu}, \quad (2.19)$$



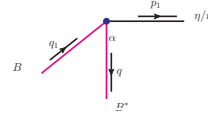
$$\bar{B} \equiv i g_{\chi_{b1} BB^*} \epsilon_{\mu\rho\alpha\beta} \epsilon_{\chi_{b2}}^{*\mu\nu} p_2^{\rho} q_{\nu} q_2^{\beta} \epsilon_{B^*}^{\alpha}, \quad (2.20)$$



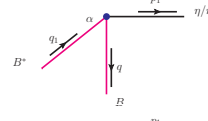
$$\bar{B}^* \equiv -i g_{\chi_{b1} BB^*} \epsilon_{\mu\rho\alpha\beta} \epsilon_{\chi_{b2}}^{*\mu\nu} p_2^{\rho} q_{\nu} q_2^{\beta} \epsilon_{B^*}^{\alpha}, \quad (2.21)$$



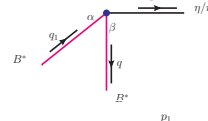
$$\bar{B}^* \equiv i g_{\chi_{b2} B^* B^*} \epsilon_{\chi_{b2}}^{*\mu\nu} \epsilon_{B^*}^{\alpha} \epsilon_{B^*}^{\beta} g_{\mu\alpha} g_{\nu\beta}, \quad (2.22)$$



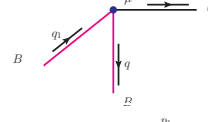
$$\bar{B} \equiv -g_{BB^* \eta^{(\prime)}} p_1^{\alpha} \epsilon_{B^*}^{\alpha}, \quad (2.23)$$



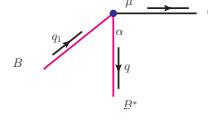
$$\bar{B}^* \equiv g_{BB^* \eta^{(\prime)}} p_1^{\alpha} \epsilon_{B^*}^{\alpha}, \quad (2.24)$$



$$\bar{B}^* \equiv -g_{B^* B^* \eta^{(\prime)}} \epsilon_{\mu\nu\alpha\beta} q_1^{\nu} q^{\mu} \epsilon_{B^*}^{\alpha} \epsilon_{B^*}^{\beta}, \quad (2.25)$$



$$\bar{B} \equiv -g_{BB\omega} \epsilon_{\omega}^{*\mu} (q_{1\mu} + q_{\mu}), \quad (2.26)$$



$$\bar{B} \equiv 2f_{BB^* \omega} \epsilon_{\mu\nu\alpha\beta} \epsilon_{\omega}^{*\mu} p_1^{\nu} (q_1^{\beta} - q^{\beta}) \epsilon_{B^*}^{\alpha}, \quad (2.27)$$

$$\begin{aligned} &\equiv 2f_{BB^*\omega}\epsilon_{\mu\nu\alpha\beta}\epsilon_{\omega}^{*\mu}P_1^\nu(q^\beta - q_1^\beta)\epsilon_{B^*}^\alpha, \quad (2.28) \\ &\equiv \epsilon_{\omega}^{*\mu}\left(g_{B^*B^*\omega}g_{\alpha\beta}(q_{1\mu} - q_\mu) + 4f_{B^*B^*\omega}\right. \\ &\quad \left.\times(g_{\mu\beta}P_{1\alpha} - g_{\mu\alpha}P_{1\beta})\right)\epsilon_{B^*}^\alpha\epsilon_{B^*}^{*\beta}. \quad (2.29) \end{aligned}$$

- [1] P. A. Zyla *et al.* [Particle Data Group], Review of Particle Physics, PTEP **2020** (2020) no.8, 083C01.
- [2] E. Kou *et al.* [Belle-II], The Belle II Physics Book, PTEP **2019** (2019) no.12, 123C01 [erratum: PTEP **2020** (2020) no.2, 029201].
- [3] R. Mizuk *et al.* [Belle], Observation of a new structure near 10.75 GeV in the energy dependence of the $e^+e^- \rightarrow \Upsilon(nS)\pi^+\pi^-$ cross sections, JHEP **10** (2019), 220.
- [4] D. Santel *et al.* [Belle], Measurements of the $\Upsilon(10860)$ and $\Upsilon(11020)$ resonances via $\sigma(e^+e^- \rightarrow \Upsilon(nS)\pi^+\pi^-)$, Phys. Rev. D **93** (2016) no.1, 011101.
- [5] D. Besson *et al.* [CLEO], Observation of New Structure in the e^+e^- Annihilation Cross-Section Above $B\bar{B}$ Threshold, Phys. Rev. Lett. **54** (1985), 381.
- [6] D. M. J. Lovelock, J. E. Horstkotte, C. Klopfenstein, J. Lee-Franzini, L. Romero, R. D. Schamberger, S. Youssef, P. Franzini, D. Son and P. M. Tuts, *et al.* Masses, Widths, and Leptonic Widths of the Higher Upsilon Resonances, Phys. Rev. Lett. **54** (1985), 377-380.
- [7] X. H. He *et al.* [Belle], Observation of $e^+e^- \rightarrow \pi^+\pi^-\pi^0\chi_{bj}$ and Search for $X_b \rightarrow \omega\Upsilon(1S)$ at $\sqrt{s} = 10.867$ GeV, Phys. Rev. Lett. **113** (2014) no.14, 142001.
- [8] A. Abdesselam *et al.* [Belle], Energy scan of the $e^+e^- \rightarrow h_b(nP)\pi^+\pi^-$ ($n = 1, 2$) cross sections and evidence for $\Upsilon(11020)$ decays into charged bottomonium-like states, Phys. Rev. Lett. **117** (2016) no.14, 142001.
- [9] J. H. Yin *et al.* [Belle], Observation of $e^+e^- \rightarrow \pi^+\pi^-\pi^0\chi_{b1,2}(1P)$ and search for $e^+e^- \rightarrow \phi\chi_{b1,2}(1P)$ at $\sqrt{s} = 10.96-11.05$ GeV, Phys. Rev. D **98** (2018) no.9, 091102.
- [10] B. Chen, A. Zhang and J. He, Bottomonium spectrum in the relativistic flux tube model, Phys. Rev. D **101** (2020) no.1, 014020.
- [11] Q. Li, M. S. Liu, Q. F. Lü, L. C. Gui and X. H. Zhong, Canonical interpretation of $Y(10750)$ and $\Upsilon(10860)$ in the Υ family, Eur. Phys. J. C **80** (2020) no.1, 59.
- [12] A. Ali, L. Maiani, A. Parkhomenko and W. Wang, Tetraquark Interpretation and Production Mechanism of the Belle $Y_b(10750)$ -Resonance, PoS **ICHEP2020** (2021), 493.
- [13] Z. G. Wang, Vector hidden-bottom tetraquark candidate: $Y(10750)$, Chin. Phys. C **43** (2019) no.12, 123102.
- [14] J. Tarrús Castellà, Spin structure of heavy-quark hybrids, AIP Conf. Proc. **2249** (2020) no.1, 020008.
- [15] J. Tarrús Castellà and E. Passeram, Exotic to standard bottomonium transitions, [arXiv:2104.03975 [hep-ph]].
- [16] P. Bicudo, M. Cardoso, N. Cardoso and M. Wagner, Bottomonium resonances with $I = 0$ from lattice QCD correlation functions with static and light quarks, Phys. Rev. D **101** (2020) no.3, 034503.
- [17] P. Bicudo, N. Cardoso, L. Müller and M. Wagner, Computation of the quarkonium and meson-meson composition of the $\Upsilon(nS)$ states and of the new $\Upsilon(10753)$ Belle resonance from lattice QCD static potentials, Phys. Rev. D **103** (2021) no.7, 074507.
- [18] W. H. Liang, N. Ikeno and E. Oset, $\Upsilon(nI)$ decay into $B^{(*)}\bar{B}^{(*)}$, Phys. Lett. B **803** (2020), 135340.
- [19] J. Segovia, P. G. Ortega, D. R. Entem and F. Fernández, Bottomonium spectrum revisited, Phys. Rev. D **93**, no.7, 074027 (2016).
- [20] J. Z. Wang, Z. F. Sun, X. Liu and T. Matsuki, Higher bottomonium zoo, Eur. Phys. J. C **78** (2018) no.11, 915.
- [21] S. Godfrey and K. Moats, Bottomonium Mesons and Strategies for their Observation, Phys. Rev. D **92** (2015) no.5, 054034.
- [22] A. M. Badalian, B. L. G. Bakker and I. V. Danilkin, On the possibility to observe higher n^3D_1 bottomonium states in the e^+e^- processes, Phys. Rev. D **79** (2009), 037505.
- [23] A. M. Badalian, B. L. G. Bakker and I. V. Danilkin, Dielectron widths of the S-, D-vector bottomonium states, Phys. Atom. Nucl. **73** (2010), 138-149.
- [24] J. L. Rosner, Charmless final states and S- and D- wave mixing in the ψ'' , Phys. Rev. D **64** (2001), 094002.
- [25] J. Z. Wang, D. Y. Chen, X. Liu and T. Matsuki, Constructing J/ψ family with updated data of charmoniumlike Y states, Phys. Rev. D **99** (2019) no.11, 114003.
- [26] J. Z. Wang, R. Q. Qian, X. Liu and T. Matsuki, Are the Y states around 4.6 GeV from e^+e^- annihilation higher charmonia?, Phys. Rev. D **101** (2020) no.3, 034001.
- [27] M. B. Voloshin, Charmonium, Prog. Part. Nucl. Phys. **61** (2008), 455-511.
- [28] M. B. Voloshin, Heavy quark spin symmetry breaking in near-threshold $J^{PC} = 1^{--}$ quarkonium-like resonances, Phys. Rev. D **85** (2012), 034024.
- [29] M. N. Anwar, Y. Lu and B. S. Zou, Heavy Quark Spin Symmetry Violating Hadronic Transitions of Higher Charmonia, PoS **Hadron2017** (2018), 100.
- [30] C. Meng and K. T. Chao, Scalar resonance contributions to the dipion transition rates of $\Upsilon(4S, 5S)$ in the re-scattering model, Phys. Rev. D **77** (2008), 074003.
- [31] C. Meng and K. T. Chao, Peak shifts due to $B^{(*)} - \bar{B}^{(*)}$ rescattering in $\Upsilon(5S)$ dipion transitions, Phys. Rev. D **78** (2008), 034022.
- [32] C. Meng and K. T. Chao, $\Upsilon(4S, 5S) \rightarrow \Upsilon(1S)\eta$ transitions in the rescattering model and the new BaBar measurement, Phys. Rev. D **78** (2008), 074001.
- [33] D. Y. Chen, J. He, X. Q. Li and X. Liu, Dipion invariant mass distribution of the anomalous $\Upsilon(1S)\pi^+\pi^-$ and $\Upsilon(2S)\pi^+\pi^-$ production near the peak of $\Upsilon(10860)$, Phys. Rev. D **84** (2011), 074006.
- [34] D. Y. Chen, X. Liu and S. L. Zhu, Charged bottomonium-like states $Z_b(10610)$ and $Z_b(10650)$ and the $\Upsilon(5S) \rightarrow \Upsilon(2S)\pi^+\pi^-$ decay, Phys. Rev. D **84** (2011), 074016.
- [35] D. Y. Chen, X. Liu and X. Q. Li, Anomalous dipion invariant mass distribution of the $\Upsilon(4S)$ decays into $\Upsilon(1S)\pi^+\pi^-$ and $\Upsilon(2S)\pi^+\pi^-$, Eur. Phys. J. C **71** (2011), 1808.
- [36] D. Y. Chen, X. Liu and T. Matsuki, Explaining the anomalous

- $\Upsilon(5S) \rightarrow \chi_{bJ}\omega$ decays through the hadronic loop effect, Phys. Rev. D **90** (2014) no.3, 034019.
- [37] B. Wang, X. Liu and D. Y. Chen, Prediction of anomalous $\Upsilon(5S) \rightarrow \Upsilon(1^3D_J)\eta$ transitions, Phys. Rev. D **94** (2016) no.9, 094039.
- [38] Q. Huang, B. Wang, X. Liu, D. Y. Chen and T. Matsuki, Exploring the $\Upsilon(6S) \rightarrow \chi_{bJ}\phi$ and $\Upsilon(6S) \rightarrow \chi_{bJ}\omega$ hidden-bottom hadronic transitions, Eur. Phys. J. C **77** (2017) no.3, 165.
- [39] Y. Zhang and G. Li, Exploring the $\Upsilon(4S, 5S, 6S) \rightarrow h_b(1P)\eta$ hidden-bottom hadronic transitions, Phys. Rev. D **97** (2018) no.1, 014018.
- [40] Q. Huang, H. Xu, X. Liu and T. Matsuki, Potential observation of the $\Upsilon(6S) \rightarrow \Upsilon(1^3D_J)\eta$ transitions at Belle II, Phys. Rev. D **97** (2018) no.9, 094018.
- [41] Q. Huang, X. Liu and T. Matsuki, Proposal of searching for the $\Upsilon(6S)$ hadronic decays into $\Upsilon(nS)$ plus $\eta^{(\prime)}$, Phys. Rev. D **98** (2018) no.5, 054008.
- [42] U. Tamponi *et al.* [Belle], First observation of the hadronic transition $\Upsilon(4S) \rightarrow \eta h_b(1P)$ and new measurement of the $h_b(1P)$ and $\eta_b(1S)$ parameters, Phys. Rev. Lett. **115** (2015) no.14, 142001.
- [43] E. Guido *et al.* [Belle], Study of η and dipion transitions in $\Upsilon(4S)$ decays to lower bottomonia, Phys. Rev. D **96** (2017) no.5, 052005.
- [44] I. Adachi *et al.* [Belle], First observation of the P -wave spin-singlet bottomonium states $h_b(1P)$ and $h_b(2P)$, Phys. Rev. Lett. **108** (2012), 032001.
- [45] Y. B. Ding, K. T. Chao and D. H. Qin, Possible effects of color screening and large string tension in heavy quarkonium spectra, Phys. Rev. D **51**, 5064-5068 (1995) [[arXiv:hep-ph/9502409](#) [hep-ph]].
- [46] B. Q. Li, C. Meng and K. T. Chao, Coupled-Channel and Screening Effects in Charmonium Spectrum, Phys. Rev. D **80**, 014012 (2009) [[arXiv:0904.4068](#) [hep-ph]].
- [47] J. F. Liu and G. J. Ding, Bottomonium Spectrum with Coupled-Channel Effects, Eur. Phys. J. C **72**, 1981 (2012) [[arXiv:1105.0855](#) [hep-ph]].
- [48] R. Q. Qian, J. Z. Wang, X. Liu and T. Matsuki, Searching for higher charmonium members in J/ψ family through reaction $e^+e^- \rightarrow \Lambda_c \bar{\Lambda}_c$, [[arXiv:2104.13270](#) [hep-ph]].
- [49] B. Q. Li and K. T. Chao, Bottomonium Spectrum with Screened Potential, Commun. Theor. Phys. **52** (2009), 653-661.
- [50] M. P. Locher, Y. Lu and B. S. Zou, Rates for the reactions $\bar{p}p \rightarrow \pi\phi$ and $\gamma\phi$, Z. Phys. A **347** (1994), 281-284.
- [51] X. Q. Li, D. V. Bugg and B. S. Zou, A Possible Explanation of the " $\rho\pi$ Puzzle" in J/Ψ , Ψ' decays, Phys. Rev. D **55** (1997), 1421-1424.
- [52] H. Y. Cheng, C. K. Chua and A. Soni, Final state interactions in hadronic B decays, Phys. Rev. D **71** (2005), 014030.
- [53] O. Gortchakov, M. P. Locher, V. E. Markushin and S. von Rotz, Two meson doorway calculation for $\bar{p}p \rightarrow \phi\pi$ including off-shell effects and the OZI rule, Z. Phys. A **353** (1996), 447-453.
- [54] X. Liu, X. Q. Zeng and X. Q. Li, Study on contributions of hadronic loops to decays of $J/\psi \rightarrow$ vector + pseudoscalar mesons, Phys. Rev. D **74** (2006), 074003.
- [55] X. Liu, B. Zhang and X. Q. Li, The Puzzle of excessive non- $D\bar{D}$ component of the inclusive $\psi(3770)$ decay and the long-distant contribution, Phys. Lett. B **675** (2009), 441-445.
- [56] G. Li, X. h. Liu, Q. Wang and Q. Zhao, Further understanding of the non- $D\bar{D}$ decays of $\psi(3770)$, Phys. Rev. D **88** (2013) no.1, 014010.
- [57] R. Casalbuoni, A. Deandrea, N. Di Bartolomeo, R. Gatto, F. Feruglio and G. Nardulli, Phenomenology of heavy meson chiral Lagrangians, Phys. Rept. **281** (1997), 145-238.
- [58] H. Xu, X. Liu and T. Matsuki, Understanding $B^- \rightarrow X(3823)K^-$ via rescattering mechanism and predicting $B^- \rightarrow \eta_c 2(^1D_2)/\psi_3(^3D_3)K^-$, Phys. Rev. D **94** (2016) no.3, 034005.
- [59] M. X. Duan, J. Z. Wang, Y. S. Li and X. Liu, The role of the newly measured $B \rightarrow K D \bar{D}$ process to establish $\chi_{c0}(2P)$ state, [[arXiv:2104.09132](#) [hep-ph]].
- [60] M. B. Wise, Chiral perturbation theory for hadrons containing a heavy quark, Phys. Rev. D **45** (1992) no.7, R2188.
- [61] F. L. Wang and X. Liu, Exotic double-charm molecular states with hidden or open strangeness and around 4.5 ~ 4.7 GeV, Phys. Rev. D **102** (2020) no.9, 094006.
- [62] F. L. Wang, R. Chen and X. Liu, Prediction of hidden-charm pentaquarks with double strangeness, Phys. Rev. D **103** (2021) no.3, 034014.
- [63] F. L. Wang, X. D. Yang, R. Chen and X. Liu, Hidden-charm pentaquarks with triple strangeness due to the $\Omega_c^{(*)}\bar{D}_s^{(*)}$ interactions, Phys. Rev. D **103** (2021) no.5, 054025.
- [64] E. V. Veliev, H. Sundu, K. Azizi and M. Bayar, Scalar Quarkonia at Finite Temperature, Phys. Rev. D **82** (2010), 056012.
- [65] D. Coffman *et al.* [MARK-III], Measurements of J/ψ Decays Into a Vector and a Pseudoscalar Meson, Phys. Rev. D **38** (1988), 2695 [erratum: Phys. Rev. D **40** (1989), 3788].
- [66] J. Jousset *et al.* [DM2], The $J/\psi \rightarrow$ Vector + Pseudoscalar Decays and the η, η' Quark Content, Phys. Rev. D **41** (1990), 1389.